SAN095-3012C

CONF-960610--4

X-RAY EMISSION FROM A HIGH-ATOMIC-NUMBER Z-PINCH PLASMA CREATED FROM COMPACT WIRE ARRAYS*

T. W. L. Sanford,[1] D. Mosher,[2] J. S. De Groot,[3] J. Hammer,[4] B. M. Marder,[1] S. Maxon,[4] T. J. Nash,[1] R. B. Spielman,[1] P. T. Springer,[4] K. Struve,[5] R. S. Thoe,[4] D. R. Welch,[5] W. E. Alley,[4] C. Bruns,[4] J. L. Eddleman,[4] J. Emic,[4] T. L. Gilliland,[1] J. Hernandez,[4] D. Jobe,[1] J. S. McGurn,[1] R. C. Mock,[1] J. F. Seamen,[1] M. Vargas,[1] and G. B. Zimmerman[4]

[1]*Sandia National Laboratories, Albuquerque, NM 87185*
[2]*Naval Research Laboratory, Washington, DC 20375*
[3]*University of California, Davis, CA 95616*
[4]*Lawrence Livermore National Laboratory, Livermore, CA 94550*
[5]*Mission Research Corporation, Albuquerque, NM 87106*

MASTER

Thermal and nonthermal x-ray emission from the implosion of compact tungsten wire arrays in 5-MA Saturn discharges is reported. The timing of multiple implosions and the thermal x-ray spectra (1 to 10 keV) agree with 2D radiation-hydrocode simulations. Nonthermal x-ray emission (10 to 100 keV) correlates with pinch spots distributed along the z-axis. The similarities of the measured nonthermal spectrum, yield, and pinch-spot emission with those of 0.8-MA, single-exploded-wire discharges on Gamble-II suggest a common nonthermal-production mechanism. Nonthemal x-ray yields are lower than expected from current scaling of Gamble II results, suggesting that implosion geometries are not as efficient as single-wire geometries for nonthermal x-ray production. The instabilities, azimuthal asymmetries, and inferred multiple implosions that accompany the implosion geometry lead to larger, more irregular pinch spots, a likely reason for reduced nonthermal efficiency. A model for nonthermal-electron acceleration across magnetic fields in highly-collisional, high-atomic-number plasmas combined with 1D hydrocode simulations of Saturn compact loads predicts weak nonthermal x-ray emission.

Intense bursts of warm x rays (10 to 100 keV) are desired for the study of in-depth material effects induced by nuclear radiation. The plasma radiation source (PRS) provides an excellent source of keV thermal x rays when the imploding plasma stagnates on the axis of symmetry, and its radial kinetic energy is converted into internal energy and radiation.[1] However, thermal radiation production from the PRS, of which Saturn is the highest-current example, drops rapidly for photon energies exceeding a few keV due to the low masses required for high temperature, and the growth of instabilities.[1] The need for x-radiation sources in the 5- to 100-keV regime between existing PRS and bremsstrahlung sources motivated the present work.

High-atomic-number z-discharge plasmas created by passing 0.8 MA through single wires on the Gamble-II generator demonstrated matched-load behavior,[2] efficient conversion of coupled electrical energy to XUV radiation, about 10% conversion to keV thermal x-ray lines and continuum,[3] and more importantly for the present work, about 0.25% conversion to non-thermal, bremsstrahlung-like lines and continuum in the 5- to 100-keV regime[4]. This and other pinch plasmas have nonthermal x-ray emission correlated with the formation of tight, x-ray-bright pinch spots.[5] The Gamble-II experiments demonstrated a Z^2 atomic-number scaling for the nonthermal radiation yield and suggested an I^2 current scaling. These scalings motivated the present Saturn experiment[6] to measure and model the x-radiation from tungsten z-pinches at order-of-magnitude higher currents than Gamble II. Saturn compact arrays were configured to resemble the nonthermal Gamble-II loads in a low-inductance geometry for efficient coupling.

The radius of the wire array was chosen such that implosions occurred early with respect to the time of nominal peak current, enabling a sausage-unstable z-pinch to form pinch spots[7] during the peak current-portion of the pulse. The array mass was chosen to recover similar values of $E/n \sim I/(m/L)$ as in Gamble II, where E is an inductive electric field, n is ion density, I is current, m and L are load mass and length.[6] Gamble-II tungsten-wire loads with strong nonthermal emission had I/(m/L) values of about 2 MA/(mg/cm).[4] Aluminum, copper, and tungsten loads of 0.5 to 8 mg were studied. For this mass scaling, a 4-mm-diameter array was

MASTER

DISTRIBUTION OF THIS DOCUMENT IS UNLIMITED DC

the lowest-inductance configuration that satisfied the early-implosion requirement. This small annular radius also insured that a small-radius pinch, similar to the Gamble-II single-wire pinches, would form. Compared to conventional PRS loads,[1] the Saturn compact pinch has an order-of-magnitude higher mass confined in a region of order-of-magnitude smaller radius and is therefore much denser and brighter.

Six B-dot probes measured the current in the MITL adjacent the insulator stack, and two B-dot probes measured the current in the radial feed adjacent to the load They were bench calibrated and intercalibrated with piezoelectric stress gauges to an accuracy of 5%. Typically, peak load currents were 5.5 MA. This current level was lower than usual for Saturn because of early implosion and the higher inductance of the compact-array. MITL currents were typically 1 MA higher, indicating significant electron-beam losses that were evidenced by strong bremsstrahlung and damage in the load region.

The temporal and spatial characteristics of the radiation were sampled by detectors at 35° from the normal to the symmetry axis so that each viewed 1.5 cm of the 2-cm plasma length. A nickel bolometer, filtered diamond photoconducting detectors (PCDs), and a filtered fluorescer array (FFA) measured the radiation output as a function of time in broad photon-energy bins ranging from 0 to ~350 keV.[6] A fast-framing x-ray pinhole camera measured the spatial distribution of the radiation in 1-to-4-keV and 4-to-10-keV energy bands in five, 3-ns frames with 5-ns dwell times. A KAP crystal spectrometer measured the time-integrated x-ray spectrum from 0.8 to 3 keV with 1-eV resolution. Owing to the broad band response of the detectors and uncertainties in x-ray spectra, the uncertainty in the measured radiation output from a PCD or FFA is about a factor of two.

Figure 1 compares the radiation measured in the bolometer (response centered at 0.4 keV), a 1-keV PCD, and a 140-keV PCD for 4-mg Al and W compact-array loads. The 140-keV channel shows a broad electron-beam-bremsstrahlung signature on top of which nonthermal radiation spikes from the plasma are visible for the tungsten load. Though x-ray yields in the sub-keV and keV regimes were comparable for Al, Cu, and W, higher-energy, nonthermal yields were consistent with the Z^2 scaling observed in Gamble-II experiments. Tungsten x-ray yields in the 10- to 100-keV regime were comparable to those measured on Gamble II at lower currents, resulting in a yield efficiency of about (0.05 ± 0.03)%.

X-radiation at all energies is characterized by multiple radiation peaks. The period between peaks grows from about 10 ns to about 40 ns as the mass is increased from 1 to 8 mg. The multiple-peak behavior is interpreted as an oscillation of plasma radius predicted by analysis[8] and radiation-MHD (RMHD) code simulations.[9] Inertia causes kinetic pressure to exceed magnetic pressure at peak compression so that the plasma expands against the magnetic field. As the plasma expands and cools, magnetic pressure again exceeds the kinetic pressure and the plasma is recompressed. The process continues until the driving

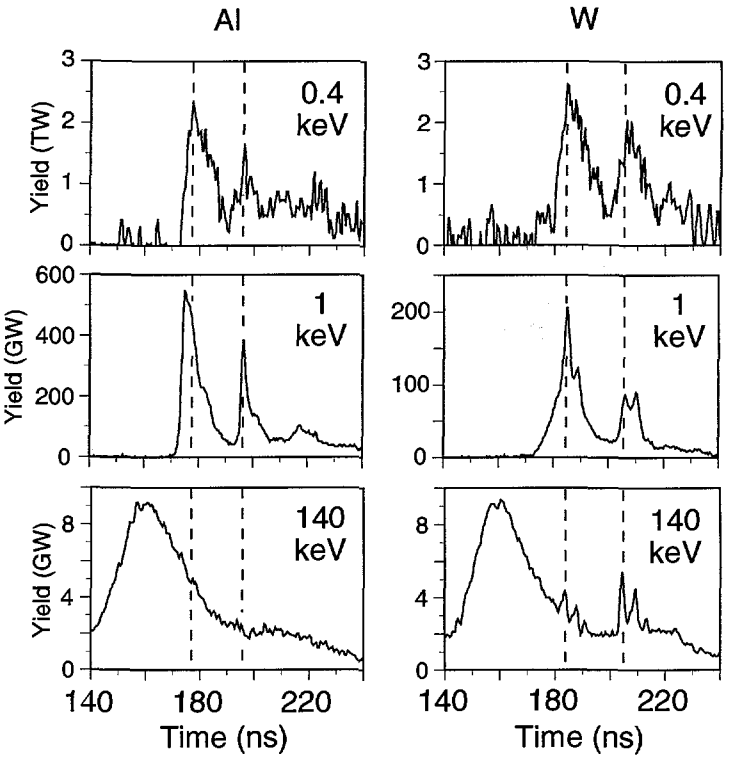

Fig. 1. Comparison of radiation measured in the bolometer (0.4 keV), 1-keV PCD, and 140-keV PCD for 4-mg Al and W loads.

current pulse decays, excess internal energy is radiated away, or instabilities terminate the oscillations. Quantitative agreement between experiment and RMHD results for the variation of bounce period with mass indicates that the current measured by the load monitors indeed flows through the plasma.

Additional support for the load-current measurements is provided by the measured variation of implosion time with load mass in Fig. 2. The circuit-model code Zork with a slug-model imploding load calculates current histories and implosion times that agree with the load monitors and x-ray diagnostics.[6] The dashed line corresponds to the implosion time for a linearly-increasing current fitted to the Saturn waveform.[6]

Figure 3 compares power-law fits to the time-integrated x-ray spectrum measured by the various diagnostics with that calculated by RMHD for a 4-mg W load. The short dashed lines show the uncertainties in the x-ray measurements. Little spectral difference is measured over masses of 1 to 4 mg. The spectrum shows a clear change in slope at about 10 keV separating thermal and nonthermal regimes. Comparison of the measured spectrum with RMHD shows that photon energies $h\nu > 12$ keV are associated with nonthermal processes not accounted for in the simulation. The slope of the measured spectrum in the 10- to 100-keV range is consistent with that measured in the Gamble-II experiment[4]: both spectra vary like $(h\nu)^{-1.4}$. This similarity indicates similar nonthermal-electron spectra in the two experiments, thereby suggesting a common nonthermal-production mechanism. However, the Gamble-II nonthermal efficiency was about three times higher than Saturn's, suggesting that an implosion geometry does not produce nonthermal x rays as efficiently as single-wire discharges. Instabilities, azimuthal asymmetries, and inferred multiple implosions that accompany the implosion geometry lead to larger, more irregular pinch spots, a likely reason for reduced nonthermal efficiency.

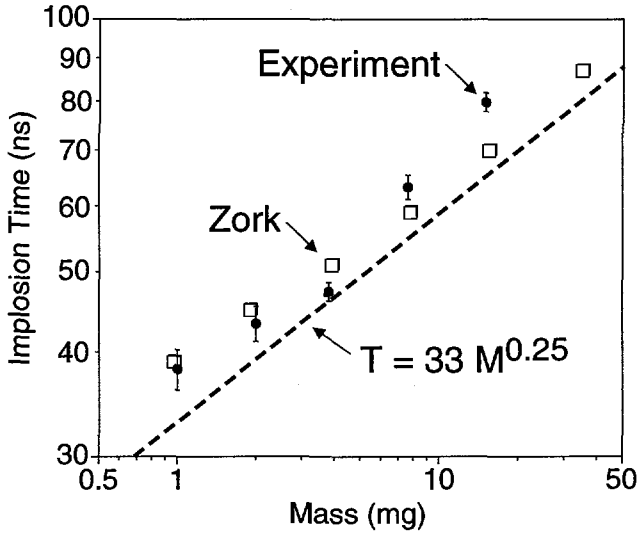

Fig. 2. Variation of measured and calculated implosion time with load mass.

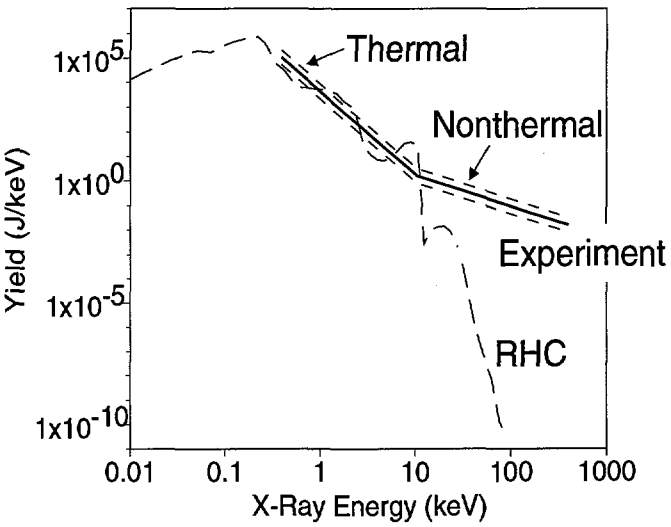

Fig. 3. Comparison of experimental power-law spectrum with that calculated by RMHD for a 4-mg tungsten load.

A fluid model for nonthermal electron acceleration in dense, high-atomic-number (high-Z) z-pinches has been developed and benchmarked against the electromagnetic, Monte-Carlo code IPROP.[6,10] In such plasmas, electrons (with initial energies in excess of a minimum value K_0) gain energy from the electric field (in excess of a critical field E_c) by cross-field scattering collisions until they reach energy K_f, an energy high enough to make them collisionless on the cyclotron-frequency time-

$$E_c(V/cm) = 3\times10^{-5}\varepsilon^{1/2}\Omega_c^{2/3}\Omega_s^{1/3}$$

$$K_0(eV) = 6\varepsilon^{1/2}\Omega_s / E$$

$$K_f(eV) = 6\times10^{14}E^2/\varepsilon\Omega_c^2$$

scale. Here, ε = 1/(Z+2), Ω_c is the electron cyclotron frequency, and Ω_s is the elastic scattering frequency for a 250-keV electron. For electric fields lower than E_c or initial electron energies below K_0, no energy gain above thermal levels is predicted. When the magnetic field approaches zero, only the K_0 equation, essentially the Dreicer runaway condition, is significant. High energies are achieved for high-Z because the scattering rate is about Z-times the energy loss rate. The particle-in-cell MHD code TIP, used to study the time-evolution of density, temperature, and electromagnetic-field radial profiles in compact-array pinches[6], calculates that peak electric fields and temperatures are at least an order-of-magnitude less than the minimum required values E_c and K_0. Therefore, strong nonthermal-electron acceleration is not predicted, in support of Saturn experimental observations.

*This work was supported by the U.S. DOE under Contract DE-AC04-94AL85000.

[1] N. R. Pereira and J. Davis, *J. Appl. Phys.* **64**, R1 (1988).
[2] D. Mosher, et al., *Ann. N. Y. Acad. Sci.* **25**, 632 (1975).
[3] C. M. Dozier, et al., *J. Phys.* **B10**, L73 (1977).
[4] D. J. Johnson, S. J. Stephanakis, and D. Mosher, NRL Memo Rep. 3207, 1976.
[5] C. Deeney, PhD. Thesis, Blackett Laboratory, Imperial College, London SW7, UK (April 1988).
[6] T. W. L. Sanford, D. Mosher, et al., Sandia Report SAND96-0222, UC-706, March 1996.
[7] D. Mosher and D. Colombant, *Phys. Rev. Lett.* **68**, 2600 (1992).
[8] D. Mosher and D. Colombant, *Dense Z-Pinches*, N. R. Pereira, J. Davis, and N. Rostoker, eds., *AIP Conf. Proc.* **195** (AIP, New York, 1989), p. 191.
[9] J. H. Hammer, et al., *Phys. Plasmas* **3**, 2063 (1996).
[10] D. R. Welch, C. L. Olson and T. W. L. Sanford, *Phys. Plasmas* **1**, 768 (1994).

DISCLAIMER

This report was prepared as an account of work sponsored by an agency of the United States Government. Neither the United States Government nor any agency thereof, nor any of their employees, makes any warranty, express or implied, or assumes any legal liability or responsibility for the accuracy, completeness, or usefulness of any information, apparatus, product, or process disclosed, or represents that its use would not infringe privately owned rights. Reference herein to any specific commercial product, process, or service by trade name, trademark, manufacturer, or otherwise does not necessarily constitute or imply its endorsement, recommendation, or favoring by the United States Government or any agency thereof. The views and opinions of authors expressed herein do not necessarily state or reflect those of the United States Government or any agency thereof.